

Decaying Sensitivity of the Zero Solution for a Class of Nonlinear Optimal Control Problems

Lars Grüne * Mario Sperl *

* *Mathematical Institute, University of Bayreuth, Bayreuth, Germany*
 (e-mail: lars.gruene@uni-bayreuth.de, mario.sperl@uni-bayreuth.de).

Abstract: We study spatial decay properties of sensitivities in a nonlinear optimal control problem with a graph-structured interaction topology. For a problem with nonlinear decoupled dynamics and quadratic cost, we show that a localized perturbation of the zero reference leads to an optimal trajectory that decays exponentially with the graph distance. The analysis, based on a nonlinear controllability condition, provides a first step toward extending known spatial decay results from linear-quadratic to nonlinear systems. A numerical example illustrates the theoretical findings.

Keywords: optimal control, interconnected nonlinear systems, decaying sensitivity, numerical methods for optimal control, large-scale systems

1. INTRODUCTION

High-dimensional optimal control problems arise naturally in a wide range of applications, including large-scale networked systems, multi-agent coordination, traffic and energy systems, and distributed robotics. In such settings, the overall system consists of a large number of interacting subsystems or agents, and the resulting state space grows proportionally with the number of components. As a consequence, classical centralized solution approaches quickly become computationally infeasible, a phenomenon commonly referred to as the curse of dimensionality (Bellman (1957)).

To address this challenge, significant effort has been devoted to the development of decentralized and distributed control strategies. A key idea underlying these approaches is that, in many large-scale systems, interactions between subsystems exhibit a localized structure: individual agents are directly influenced only by a limited subset of other agents, for instance, through spatial proximity or network connections. Exploiting such locality properties is essential for reducing computational complexity and enabling scalable control designs.

From a theoretical perspective, this raises the fundamental question of how perturbations or changes in the state of one subsystem affect the optimal behavior of other subsystems. In particular, understanding the sensitivity of optimal trajectories and value functions with respect to localized perturbations is crucial for justifying decentralized approximations and localized solution methods. If the influence of a perturbation decays sufficiently fast with respect to an appropriate notion of distance between

subsystems, then the global optimal control problem may be well approximated by considering only localized subproblems.

Motivated by these considerations, recent research has focused on sensitivity analysis and spatial decay properties in large-scale optimal control problems. In Sperl et al. (2023, 2025), a separable approximation of the optimal value function is constructed based on a spatial decay property of sensitivities between subsystems. This property enables an efficient representation of the optimal value function using separable structured neural networks. A crucial ingredient for the scalability of the approach is that the sensitivity decay holds uniformly with respect to the system dimension. A natural objective is therefore to identify control-theoretic conditions that guarantee uniform spatially decaying sensitivity.

Building on earlier work on spatial decay phenomena in graph-structured nonlinear optimization problems (see Shin et al. (2022)), the paper Shin et al. (2023) establishes an exponential decay of the optimal feedback matrix for time-discrete linear-quadratic optimal control problems under stabilizability and detectability assumptions. Complementary to this line of work, Zhang et al. (2023) shows that the entries of the optimal feedback matrix decay exponentially, assuming that the system matrices exhibit a corresponding decay structure. We emphasize that all these results require linearity of the dynamics.

Further notions of decay and sensitivity have been investigated in other contexts. Spatial decay of sensitivities has also been studied for optimal control problems governed by partial differential equations and more general evolution equations, see Göttlich et al. (2025a,b); Oppeneiger et al. (2025). Exponential decay with respect to time, rather than space, is for example analyzed in Shin and Zavala (2021); Na and Anitescu (2020); Grüne et al. (2020). Moreover, scalable reinforcement learning methods exploiting

* The authors thank Andrii Mironchenko, Manuel Schaller, and Karl Worthmann for valuable discussions and helpful comments. This work was funded by the Deutsche Forschungsgemeinschaft (DFG, German Research Foundation) - project number 463912816.

exponential decay properties of the Q -function are proposed in Qu et al. (2022).

In this work, we establish spatial decay properties of sensitivities for a class of finite-dimensional nonlinear optimal control problems under an asymptotic controllability assumption. Our result can be viewed as a first step toward a nonlinear extension of the sensitivity decay results for linear-quadratic optimal control problems obtained in Shin et al. (2023). In contrast to the linear-quadratic setting of Shin et al. (2023), where the analysis relies on matrix-based arguments, the nonlinear nature of the problem necessitates a fundamentally different proof technique. In order to derive decay properties without resorting to localization arguments, we introduce a controllability condition tailored to the nonlinear setting. To focus on this core mechanism, we consider a simplified yet nontrivial class of problems with nonlinear but decoupled dynamics and a quadratic cost functional, and analyze the decay of sensitivities of the zero solution.

The outline of the paper is as follows. After introducing the problem setting in the next section, Section 3 presents the main theorem. Its proof is given in Section 4. A numerical test case is discussed in Section 5, and the paper concludes with Section 6.

2. SETTING

2.1 Dynamics and Norm Conventions

We consider decoupled nonlinear dynamics

$$\dot{x}_i = f_i(x_i, u_i) \quad (1)$$

with $i = 1, \dots, s$, where the vector fields $f_i: \mathbb{R}^{n_i} \times \mathbb{R}^{m_i} \rightarrow \mathbb{R}^{n_i}$ satisfy $f_i(0, 0) = 0$ for all i . The initial conditions at time $t = 0$ are denoted by $x_{0,i}$. The aggregated state and control vectors are given by

$$x = \begin{pmatrix} x_1 \\ \vdots \\ x_s \end{pmatrix} \in \mathbb{R}^n, u = \begin{pmatrix} u_1 \\ \vdots \\ u_s \end{pmatrix} \in \mathbb{R}^m,$$

where $n = \sum_{i=1}^s n_i$, and $m = \sum_{i=1}^s m_i$.

We consider a set of initial values $\Omega \subseteq \mathbb{R}^n$ containing a neighborhood of the origin and assume that the system (1) is forward complete, i.e., for any $x_0 \in \Omega$ and for any input u the corresponding solution of (1) exists and is unique for all nonnegative times. We denote it by $x(\cdot, x_0, u)$.

Further, for an index set $\mathcal{I} \subseteq \{1, \dots, s\}$ we denote by $x_{\mathcal{I}} \in \mathbb{R}^{n_{\mathcal{I}}}$ and $u_{\mathcal{I}} \in \mathbb{R}^{m_{\mathcal{I}}}$ the vectors that comprise the states and control from all subsystems in \mathcal{I} , respectively, with $n_{\mathcal{I}} := \sum_{i \in \mathcal{I}} n_i$ and $m_{\mathcal{I}} := \sum_{i \in \mathcal{I}} m_i$. We endow \mathbb{R}^n with the norm

$$\|x\| = \left(\sum_{i=1}^s |x_i|^2 \right)^{1/2},$$

where each $|\cdot|$ denotes a fixed (but otherwise arbitrary) norm on \mathbb{R}^{n_i} . For any index set $\mathcal{I} \subseteq \{1, \dots, s\}$ we use the same convention for the subvectors $x_{\mathcal{I}}$ of x , i.e.,

$$\|x_{\mathcal{I}}\| = \left(\sum_{i \in \mathcal{I}} |x_i|^2 \right)^{1/2}.$$

This norm satisfies two elementary properties that will be used repeatedly in the following. First, for any function

$x: \mathbb{R}_{\geq 0} \rightarrow \mathbb{R}^n$, its squared L_2 -norm decomposes componentwise:

$$\begin{aligned} \|x\|_{L_2}^2 &= \int_0^\infty \|x(t)\|^2 dt = \int_0^\infty \sum_{i=1}^s |x_i(t)|^2 dt \\ &= \sum_{i=1}^s \int_0^\infty |x_i(t)|^2 dt = \sum_{i=1}^s \|x_i\|_{L_2}^2. \end{aligned}$$

Second, if $\mathcal{I}_1 \subseteq \mathcal{I}_2 \subseteq \{1, \dots, s\}$ are index sets, then monotonicity with respect to the index set holds:

$$\|x_{\mathcal{I}_1}\| \leq \|x_{\mathcal{I}_2}\|.$$

The same monotonicity property applies to the associated L_2 -norms of time-dependent functions.

2.2 Optimal Control Problem

The subsystems (1) are coupled via quadratic costs

$$\ell(x, u) = \sum_{i,j=1}^s x_i^T Q_{ij} x_j + \sum_{k=1}^s u_k^T R_k u_k = x^T Q x + u^T R u, \quad (2)$$

where Q and R are assumed to be symmetric and positive definite. Hence, there exist constants $\mu, M_Q, M_R > 0$ such that for all $x \in \mathbb{R}^n$

$$\mu \|x\|^2 \leq x^T Q x, \quad \|Qx\| \leq M_Q \|x\|, \quad \|Rx\| \leq M_R \|x\|. \quad (3)$$

We consider the infinite horizon optimal control problem of minimizing the cost functional

$$J(x_0, u) = \int_0^\infty \ell(x(t, x_0, u), u(t)) dt \quad (4)$$

over all admissible controls $u \in \mathcal{U} = L_\infty([0, \infty), U)$, $U \subseteq \mathbb{R}^m$, for a given initial value $x_0 \in \Omega$. We assume that for every initial value $x_0 \in \Omega$ there exists an optimal control $u^* \in \mathcal{U}$ such that

$$J(x_0, u^*) = \inf_{u \in \mathcal{U}} J(x_0, u).$$

If the optimal control is not unique, u^* is understood to denote a fixed representative. We denote the corresponding optimal trajectory via $x^*(\cdot) = x(\cdot, x_0, u^*)$. If this assumption is not satisfied, we expect that the following results can be extended to nearly optimal trajectories; however, we leave a rigorous analysis of this case for future work.

While the dynamics of the subsystems in (1) are decoupled, the overall optimal control problem with cost functional J defined in (4) introduces a coupling through the matrix Q in (2). We represent this interconnection of the subsystems by an undirected graph $\mathcal{G} = (\mathcal{V}, \mathcal{E})$, where each subsystem corresponds to a node identified with its index, i.e., we set $\mathcal{V} = \{1, \dots, s\}$. For each pair of distinct nodes $i \neq j$, the unordered pair $\{i, j\}$ is an edge in the graph if and only if $Q_{ij} \neq 0$ (which, by the symmetry of Q , is equivalent to $Q_{ji} \neq 0$). The graph distance between two nodes is defined as the length of the shortest path connecting them and is denoted by $d_{\mathcal{G}}(i, j)$. Note that $d_{\mathcal{G}}(i, j) \geq 2$ for $i \neq j$ if and only if $Q_{ij} = 0$. For a nonempty subset $\mathcal{W} \subseteq \mathcal{V}$ and a node $i \in \mathcal{V}$, we define $d_{\mathcal{G}}(i, \mathcal{W}) = \min_{j \in \mathcal{W}} d_{\mathcal{G}}(i, j)$.

In the following, we refer to the setting introduced in this subsection as an optimal control problem (OCP) of the form (1) - (4).

2.3 Problem Formulation

Note that from the assumptions on f_i , Q , and R it immediately follows that $x^*(t) \equiv 0$ with control $u^*(t) \equiv 0$ is the optimal solution for the initial condition $x_0 = 0$. In this paper, we investigate how the solution changes across the different subsystems if a single subsystem has a nonzero initial value $x_{0,i^*} \neq 0$ while all other initial values remain 0. Our aim is to quantify how this influence propagates through the network, with an estimate that reflects the distance of each subsystem from i^* and remains independent of the overall dimension, i.e., independent of s and n_i , and thus also independent of n .

3. MAIN RESULT

To formulate our main result on sensitivity decay, we impose the following assumption of asymptotic controllability to the origin for a system of equations (1).

Assumption 1. There are $C, \sigma > 0$, such that for each $x_0 \in \Omega$ there is a control $u_{x_0} \in \mathcal{U}$ such that for all $t \geq 0$ the inequalities

$$\|x(t, x_0, u_{x_0})\| \leq Ce^{-\sigma t}\|x_0\|, \|u_{x_0}(t)\| \leq Ce^{-\sigma t}\|x_0\| \quad (5)$$

hold.

Given this assumption, the main result guarantees that the sensitivity of the zero solution decreases exponentially as a function of the distance in the underlying graph of subsystems. In the following, for $a \in \mathbb{R}$, we write $\lceil a \rceil$ for the smallest integer greater than or equal to a .

Theorem 2. Consider an OCP of the form (1)-(4) satisfying Assumption 1. Pick any $i^* \in \mathcal{V}$ and let the initial value $x_0 \in \Omega$ be such that $x_{0,i^*} \neq 0$ and $x_{0,i} = 0$ for all $i \neq i^*$. Denote the optimal trajectory starting at x_0 by x^* . Then for any subset $\mathcal{W} \subseteq \mathcal{V}$, the norm of the optimal trajectories of the subsystems in \mathcal{W} satisfies

$$\|x_{\mathcal{W}}^*\|_{L_2} \leq S \rho^{d_{\mathcal{G}}(i^*, \mathcal{W})} |x_{0,i^*}|, \quad (6)$$

where $S = 2 \max\{C_{\text{init}}, C_{\text{prop}}\}$, $\rho = 2^{-1/q} < 1$, $q = \lceil S \rceil^2$, and

$$C_{\text{init}} = \sqrt{\frac{M_Q + M_R}{2\sigma\mu}} C, \quad C_{\text{prop}} = 2M_Q\mu^{-1}.$$

Observe that for the particular case where $\mathcal{W} = \{j\}$ for some $j \in \mathcal{V}$, Theorem 2 states that the norm of the solution in subsystem j diminishes exponentially with respect to the distance of the nodes i^* and j in the graph. In other words, distant subsystems are affected only weakly by a local perturbation of the initial condition and the effect of a perturbation is concentrated near its origin.

Remark 3. (Dimension-Independent Bounds). For the application of Theorem 2 to high-dimensional optimal control problems, it is desirable that the constants appearing in the estimate (6) are independent of the state-space dimension. Examining the quantities on which the constants S and ρ in Theorem 2 depend, we observe that this can be achieved by imposing two uniformity requirements. First, the controllability condition in Assumption 1 is required to hold uniformly with respect to the dimension. Second, the constants μ , M_Q , and M_R from (3) are required to be bounded independently of the dimension. The assumption

of dimension-independent bounds on M_R and M_Q appears reasonable in the present setting. Indeed, the matrix R is assumed to be block-diagonal, which naturally yields a uniform bound on M_R . Moreover, sparsity of the cost matrix Q is an intrinsic feature of the problem formulation. If Q were fully occupied, every pair of nodes in the underlying graph would be directly coupled, in which case the notion of exponential decay with respect to graph distance would no longer be meaningful. Finally, the requirement that the matrix Q is positive definite is an assumption that we aim to weaken in future research.

4. PROOF OF THE MAIN RESULT

In this section, we prove Theorem 2. Throughout, we consider an optimal control problem of the form (1)-(4), and all statements are understood with respect to this setting. The proof is based on two auxiliary bounds on the norms of optimal trajectories, which are established in Subsections 4.1 and 4.2 and subsequently combined in Subsection 4.3.

4.1 Influence of the initial perturbation

We begin by estimating how a perturbation of the initial value $x_0 = 0$ in one component, i.e. setting $x_{0,i^*} \neq 0$ for some $i^* \in \mathcal{V}$, affects the norm of the optimal trajectory of the overall system.

Lemma 4. Let $i^* \in \mathcal{V}$. Consider an initial value $x_0 \in \Omega$ with $x_{0,i^*} \neq 0$ and $x_{0,i} = 0$ for all $i \neq i^*$ and denote the optimal trajectory starting at x_0 by x^* . Let Assumption 1 hold. Then the inequality

$$\|x^*\|_{L_2} \leq C_{\text{init}} |x_{0,i^*}|$$

holds with $C_{\text{init}} = \sqrt{\frac{M_Q + M_R}{2\sigma\mu}} C$.

Proof. Observe that $\|x_0\| = |x_{0,i^*}|$, as all other components of x_0 equal 0. Hence, from Assumption 1 we know that there exists $C, \sigma > 0$ and $u_{x_0} \in \mathcal{U}$ such that for all $t \geq 0$ the estimates (5) hold. This implies that

$$\begin{aligned} J(x_0, u_{x_0}) &= \int_0^\infty \ell(x(t, x_0, u_{x_0}), u_{x_0}(t)) dt \\ &= \int_0^\infty x(t, x_0, u_{x_0})^T Q x(t, x_0, u_{x_0}) + u_{x_0}(t)^T R u_{x_0}(t) dt \\ &\leq \int_0^\infty (M_Q + M_R) C^2 e^{-2\sigma t} |x_{0,i^*}|^2 dt \\ &= \frac{(M_Q + M_R) C^2}{2\sigma} |x_{0,i^*}|^2. \end{aligned}$$

Since the optimal control u^* generating the optimal trajectory x^* minimizes J , it follows that

$$J(x_0, u^*) = \int_0^\infty \ell(x^*(t), u^*(t)) dt \leq \frac{(M_Q + M_R) C^2}{2\sigma} |x_{0,i^*}|^2.$$

Moreover, by (3) we have that

$$\begin{aligned} \|x^*\|_{L_2}^2 &= \int_0^\infty \|x^*(t)\|^2 dt \\ &\leq \frac{1}{\mu} \int_0^\infty x^*(t)^T Q x^*(t) dt \leq \frac{1}{\mu} J(x_0, u^*). \end{aligned}$$

The combination of these inequalities yields the assertion after taking the square root. \square

Note that the proof of Lemma 4 does not rely on the specific structure of the considered dynamics in (1); it only requires the matrix bounds in (3) and the controllability condition in Assumption 1. The particular structure of the dynamics will, however, be needed in the following subsection.

4.2 Propagation of error perturbation

Lemma 4 has shown how an initial perturbation affects the optimal solution. In order to see how the resulting perturbation propagates through the graph, we need a second lemma, which we provide in this subsection.

Consider two index sets $\mathcal{I}, \mathcal{J} \subseteq \mathcal{V}$, $\mathcal{I} \cap \mathcal{J} = \emptyset$, and fix some functions $\hat{x}_j: \mathbb{R}_{\geq 0} \rightarrow \mathbb{R}^{n_j}$ for all nodes $j \in \mathcal{J}$. These functions may be interpreted as externally prescribed (or perturbed) trajectories, and our goal is to quantify how such perturbations influence the optimal trajectories associated with the nodes in \mathcal{I} . To this end, we define

$$\begin{aligned} \ell_{\mathcal{I}}(x_{\mathcal{I}}, u_{\mathcal{I}}, x_{\mathcal{J}}) &= \underbrace{\sum_{j \in \mathcal{J}, i \in \mathcal{I}} (x_i^T Q_{ij} x_j + x_j^T Q_{ji} x_i)}_{=: \ell_1(x_{\mathcal{I}}, x_{\mathcal{J}})} \\ &+ \underbrace{\sum_{i, i' \in \mathcal{I}} x_i^T Q_{ii'} x_{i'}}_{=: \ell_2(x_{\mathcal{I}})} + \underbrace{\sum_{i \in \mathcal{I}} u_i^T R_i u_i}_{=: \ell_3(u_{\mathcal{I}})} \end{aligned}$$

and denote by $J_{\mathcal{I}}$ the corresponding infinite horizon functional

$$J_{\mathcal{I}}(x_{\mathcal{I},0}, u_{\mathcal{I}}, \hat{x}_{\mathcal{J}}) = \int_0^\infty \ell_{\mathcal{I}}(x_{\mathcal{I}}(t), x_{\mathcal{I},0}, u_{\mathcal{I}}(t), \hat{x}_{\mathcal{J}}(t)) dt.$$

The resulting reduced OCP then takes the form

$$\begin{aligned} \min_{u_{\mathcal{I}}} J_{\mathcal{I}}(x_{\mathcal{I},0}, u_{\mathcal{I}}, \hat{x}_{\mathcal{J}}), \\ \text{s.t. } \dot{x}_i = f_i(x_i, u_i), i \in \mathcal{I}. \end{aligned} \quad (7)$$

The following Lemma estimates the norm of the optimal solution of (7) in dependence of the norm of the fixed functions $\hat{x}_{\mathcal{J}}$.

Lemma 5. Let $\mathcal{I}, \mathcal{J} \subseteq \mathcal{V}$ be disjoint index sets. For fixed functions $\hat{x}_{\mathcal{J}}$, consider the reduced OCP (7) with initial condition $x_{\mathcal{I},0} = 0$. Then the optimal solution $\tilde{x}_{\mathcal{I}}^*$ of (7) satisfies

$$\|\tilde{x}_{\mathcal{I}}^*\|_{L_2} \leq C_{\text{prop}} \|\hat{x}_{\mathcal{J}}\|_{L_2}$$

with $C_{\text{prop}} = 2M_Q\mu^{-1}$.

Proof. Inserting $u_{\mathcal{I}}^0 \equiv 0$, we obtain that $x_{\mathcal{I}}(t, x_{\mathcal{I},0}, u_{\mathcal{I}}^0) \equiv 0$ and thus by the definition of $\ell_{\mathcal{I}}$

$$J_{\mathcal{I}}(x_{\mathcal{I},0}, u_{\mathcal{I}}^0, \hat{x}_{\mathcal{J}}) = 0.$$

Denoting the optimal control for (7) with initial value 0 by $\tilde{u}_{\mathcal{I}}^*$, this implies that

$$J_{\mathcal{I}}(x_{\mathcal{I},0}, \tilde{u}_{\mathcal{I}}^*, \hat{x}_{\mathcal{J}}) \leq 0. \quad (8)$$

Since R is positive definite, we have $\ell_3(\tilde{u}_{\mathcal{I}}^*(t)) \geq 0$ for all t . Thus, from (8) we can conclude that

$$\int_0^\infty \ell_1(\tilde{x}_{\mathcal{I}}^*(t), \hat{x}_{\mathcal{J}}(t)) + \ell_2(\tilde{x}_{\mathcal{I}}^*(t)) dt \leq 0. \quad (9)$$

Next we observe that if we take a vector $x_{\mathcal{I}} \in \mathbb{R}^{n_{\mathcal{I}}}$ and extend it to a vector $x \in \mathbb{R}^n$ by setting $x_k = 0$ for all $k \in \mathcal{V} \setminus \mathcal{I}$, we obtain that

$$\ell_2(x_{\mathcal{I}}) = \ell(x, 0) \geq \mu \|x\|^2 = \mu \|x_{\mathcal{I}}\|^2.$$

By extending $\hat{x}_{\mathcal{J}} \in \mathbb{R}^{n_{\mathcal{J}}}$ to a vector $\hat{x} \in \mathbb{R}^n$ in the same way, we get

$$\begin{aligned} \ell_1(x_{\mathcal{I}}, \hat{x}_{\mathcal{J}}) &= x^T Q \hat{x} + \hat{x}^T Q x \\ &\geq -2M_Q \|x\| \|\hat{x}\| = -2M_Q \|x_{\mathcal{I}}\| \|\hat{x}_{\mathcal{J}}\|. \end{aligned}$$

Together with (9) this yields

$$\begin{aligned} &\int_0^\infty -2M_Q \|\tilde{x}_{\mathcal{I}}^*(t)\| \|\hat{x}_{\mathcal{J}}(t)\| + \mu \|\tilde{x}_{\mathcal{I}}^*(t)\|^2 dt \\ &\leq \int_0^\infty \ell_1(\tilde{x}_{\mathcal{I}}^*(t), \hat{x}_{\mathcal{J}}(t)) + \ell_2(\tilde{x}_{\mathcal{I}}^*(t)) dt \leq 0. \end{aligned} \quad (10)$$

Now Young's inequality states that $\|\tilde{x}_{\mathcal{I}}^*(t)\| \|\hat{x}_{\mathcal{J}}(t)\| \leq \gamma \|\tilde{x}_{\mathcal{I}}^*(t)\|^2/2 + \|\hat{x}_{\mathcal{J}}(t)\|^2/(2\gamma)$ for each $\gamma > 0$ and $t \geq 0$. From (10) we can thus conclude

$$\int_0^\infty -M_Q \gamma \|\tilde{x}_{\mathcal{I}}^*(t)\|^2 - M_Q \|\hat{x}_{\mathcal{J}}(t)\|^2/\gamma + \mu \|\tilde{x}_{\mathcal{I}}^*(t)\|^2 dt \leq 0,$$

which yields

$$(\mu - M_Q \gamma) \|\tilde{x}_{\mathcal{I}}^*\|_{L_2}^2 \leq \frac{M_Q}{\gamma} \|\hat{x}_{\mathcal{J}}\|_{L_2}^2.$$

Choosing $\gamma = \mu/(2M_Q)$ this implies

$$\|\tilde{x}_{\mathcal{I}}^*\|_{L_2}^2 \leq \frac{4M_Q^2}{\mu^2} \|\hat{x}_{\mathcal{J}}\|_{L_2}^2,$$

which yields the assertion after taking the square root. \square

In the next subsection, we apply Lemma 5 in the following setting. We first solve the overall OCP (1) - (4) and then choose \hat{x}_j as the corresponding optimal trajectories, that is, $\hat{x}_j = x_j^*$ for $j \in \mathcal{J}$. The lemma below states that, under the assumption that every connection originating from a node in \mathcal{I} leads to a node contained in $\mathcal{I} \cup \mathcal{J}$, the optimal solution $\tilde{x}_{\mathcal{I}}^*$ of the reduced OCP (7) coincides¹ with $x_{\mathcal{I}}^*$, i.e., with the components of the overall optimal solution belonging to the nodes in \mathcal{I} .

Lemma 6. Consider an OCP of the form (1)-(4) with optimal solution x^* . Further, let $\mathcal{I}, \mathcal{J} \subseteq \mathcal{V}$, $\mathcal{I} \cap \mathcal{J} = \emptyset$, be two disjoint index sets which satisfy

$$\forall j \in \mathcal{V}: d_{\mathcal{G}}(j, \mathcal{I}) = 1 \implies j \in \mathcal{J}. \quad (11)$$

For $j \in \mathcal{J}$ set $\hat{x}_j = x_j^*$. Then $x_{\mathcal{I}}^*$ is an optimal solution of the reduced OCP (7).

Proof. From (11) we obtain that for any node $k \notin (\mathcal{I} \cup \mathcal{J})$ it holds that $d_{\mathcal{G}}(k, \mathcal{I}) \geq 2$, which, by the definition of \mathcal{G} implies $Q_{i,k} = Q_{k,i} = 0$ for all $i \in \mathcal{I}$. Thus, the cost function $\ell_{\mathcal{I}}$ in (7) contains all terms of ℓ in (2) that involve nodes $i \in \mathcal{I}$. Hence, the remaining terms in ℓ depend only on nodes in $\mathcal{V} \setminus \mathcal{I}$ and are thus not affected by the minimization of $J_{\mathcal{I}}$. As a consequence, if there existed a solution with a lower value of $J_{\mathcal{I}}$ than $x_{\mathcal{I}}^*$, then combining this solution with $x_{\mathcal{G} \setminus \mathcal{I}}^*$ —which by the decoupled dynamics (1) yields a feasible trajectory of the overall system—would result in a solution with a lower value of J than x^* . This would contradict the optimality of x^* .

4.3 Proof of Theorem 2

We are now in a position to combine the results from the previous subsections to establish the proof of Theorem 2.

¹ In case the optimal solutions are not unique, “coincide” is to be understood in the following sense: for each optimal solution of the overall problem there exists a solution of the reduced problem whose components for $i \in \mathcal{I}$ coincide, and vice versa.

Proof. [Theorem 2] For $k \in \mathbb{N}$ we define the sets

$$V_k := \{i \in \mathcal{V} \mid d_{\mathcal{G}}(i, i^*) \geq k\}$$

and

$$W_k := \{i \in \mathcal{V} \mid d_{\mathcal{G}}(i, i^*) = k\}.$$

We first prove the inequality

$$\|x_{V_{qk}}\|_{L_2} \leq \hat{S} \hat{\rho}^k |x_{0,i^*}|, \quad (12)$$

for $\hat{\rho} = 1/2$, $\hat{S} = \max\{C_{\text{init}}, C_{\text{prop}}\}$ and q from the statement of the theorem by induction over k . Note that we only need to carry out the induction until qk exceeds the largest distance of a node in the graph from node i^* (since otherwise V_{qk} is empty), but since this distance is arbitrarily large, we prove the induction step for an arbitrary k .

For $k = 0$ we can use Lemma 4 to obtain the inequality

$$\|x_{V_0}^*\|_{L_2} = \|x^*\|_{L_2} \leq C_{\text{init}} |x_{0,i^*}|,$$

which proves (12) for $k = 0$ since $\hat{S} \geq C_{\text{init}}$.

For the induction step $k \rightarrow k+1$, the induction assumption is that (12) holds for some k . Then we obtain

$$\sum_{k' \geq qk} \|x_{W_{k'}}\|_{L_2}^2 = \|x_{V_{qk}}\|_{L_2}^2 \leq (\hat{S} \hat{\rho}^k |x_{0,i^*}|)^2. \quad (13)$$

This implies that there is $k^* \in \{qk, qk+1, \dots, qk+q-1\}$ such that

$$\|x_{W_{k^*}}\|_{L_2} \leq \hat{\rho}^{k+1} |x_{0,i^*}|. \quad (14)$$

This holds, because otherwise

$$\sum_{k'=qk}^{q(k+1)-1} \|x_{W_{k'}}\|_{L_2}^2 > q(\hat{\rho}^{k+1} |x_{0,i^*}|)^2 \geq (\hat{S} \hat{\rho}^k |x_{0,i^*}|)^2,$$

which contradicts (13).

We now choose $\mathcal{J} = W_{k^*}$, $\mathcal{I} = V_{k^*+1}$, and set $\hat{x}_j = x_j^*$ for all $j \in \mathcal{J}$. Note that this choice of \mathcal{I} and \mathcal{J} satisfies the condition (11) of Lemma 6. Hence, applying Lemma 5 and Lemma 6 together with (14) yields

$$\begin{aligned} \|x_{V_{k^*+1}}^*\|_{L_2} &= \|x_{\mathcal{I}}^*\|_{L_2} \leq C_{\text{prop}} \|\hat{x}_{\mathcal{J}}\|_{L_2} \\ &= C_{\text{prop}} \|\hat{x}_{W_{k^*}}\|_{L_2} \leq C_{\text{prop}} \hat{\rho}^{k+1} |x_{0,i^*}|. \end{aligned}$$

Since $k^* \leq qk + q - 1$ and the V_k are decreasing with increasing k , the same inequality holds for $\|x_{V_{qk+q}}^*\|_{L_2}$. As $qk + q = q(k+1)$, this yields (12) for $k+1$ and thus proves the induction step.

Now (12) implies

$$\|x_{V_p}^*\|_{L_2} \leq \hat{S} \hat{\rho}^{p/q} |x_{0,i^*}|$$

for any $p \in \mathbb{N}$ being a multiple of q . For each such p and all $k \in \{p+1, \dots, p+q-1\}$ we obtain

$$\begin{aligned} \|x_{V_k}^*\|_{L_2} &\leq \|x_{V_p}^*\|_{L_2} \leq \hat{S} \hat{\rho}^{p/q} |x_{0,i^*}| = \hat{S} \hat{\rho}^{k/q} \hat{\rho}^{(p-k)/q} |x_{0,i^*}| \\ &= \hat{S} \hat{\rho}^k |x_{0,i^*}| \leq 2\hat{S} \hat{\rho}^k |x_{0,i^*}| = \hat{S} \hat{\rho}^k |x_{0,i^*}|. \end{aligned}$$

This shows the assertion, since for any $\mathcal{W} \subseteq \mathcal{V}$ defining $k := \rho^{\text{d}_{\mathcal{G}}(i^*, \mathcal{W})}$ yields $\mathcal{W} \subseteq V_k$ and thus $\|x_{\mathcal{W}}^*\|_{L_2} \leq \|x_{V_k}\|_{L_2}$.

5. NUMERICAL EXPERIMENT

In this section, we numerically illustrate the theoretical findings of Theorem 2. We consider a group of $s \in \mathbb{N}$ vehicles. Each vehicle is modeled as a two-dimensional system with state $x_i = (y_i, v_i) \in \mathbb{R}^2$, $i \in \mathcal{V}$, where y_i

and v_i denote the position and velocity of the i -th vehicle, respectively. The resulting state dimension is therefore $n = 2s$.

The dynamics of each vehicle are based on a double-integrator model, augmented by viscous and quadratic drag terms, and are given by

$$\dot{x}_i = f_i(y_i, u_i) = \begin{bmatrix} v_i \\ -\beta v_i - \kappa v_i |v_i| + u_i \end{bmatrix}$$

where $\beta, \kappa \in \mathbb{R}_{\geq 0}$ are fixed parameters and u_i denotes the control input of vehicle i . Such quadratic drag terms have, for instance, been used in Ray and Fröhlich (2015) and in Example 7.1 of Slotine and Li (1991) to model motions in fluids.

The control objective is to stabilize a chain of vehicles at the origin while penalizing deviations between neighboring vehicles. This reflects the goal of bringing all vehicles to rest while maintaining coherence of the formation and leads to the cost functional

$$J(x, u) = \int_0^\infty \sum_{i=1}^s y_i^2 + \gamma v_i^2 + \sum_{i=1}^{s-1} (y_{i+1} - y_i)^2 + \delta \|u\|_2^2 dt,$$

where $\gamma, \delta \in \mathbb{R}_{>0}$. We can write J in the form (4) with the cost function ℓ as in (2) by setting $R = \delta I_s$ and

$$Q = \begin{bmatrix} 3 & 0 & -1 & 0 & \dots \\ 0 & \gamma & 0 & 0 & \dots \\ -1 & 0 & 3 & 0 & -1 \\ 0 & 0 & 0 & \gamma & 0 \\ \vdots & \vdots & & \ddots & \end{bmatrix} - e_1 e_1^T - e_{n-1} e_{n-1}^T \in \mathbb{R}^{n \times n},$$

where $e_i \in \mathbb{R}^n$ denotes the i -th canonical unit vector.

The corresponding graph \mathcal{G} contains one node for each vehicle and has a sequential structure, as illustrated in Figure 1, where each vehicle is connected to its immediate predecessor and successor.



Fig. 1. Graph for $s = 5$ vehicles.

Note that, overall, this yields an OCP of the form (1)-(4) with decoupled dynamics and coupling introduced through the matrix Q . Moreover, it can be shown that Assumption 1 is satisfied for a bounded domain $\Omega \subset \mathbb{R}^n$ of initial values. By choosing feedback functions $u_i = F_i(x_i) = -y_i + \kappa v_i |v_i|$ we obtain the linear closed-loop system

$$\dot{x}_i = \begin{pmatrix} 0 & 1 \\ -1 & -\beta \end{pmatrix} x_i$$

for each vehicle $i \in \mathcal{V}$, which is exponentially stable for any $\beta > 0$. Thus, there exist $C, \sigma > 0$ such that for all $x_{0,i} \in \mathbb{R}^2$ we have $\|x_i(t, x_{0,i}, u_i)\| \leq C e^{-\sigma t} \|x_{0,i}\|$. It follows that

$$\begin{aligned} |u_i(t)| &= | -y_i(t) + \kappa v_i(t) | v_i(t) | \\ &\leq (C + \kappa C^2 \sup_{x \in \Omega} \|x\|) e^{-\sigma t} \|x_{0,i}\|, \end{aligned}$$

which verifies Assumption 1 by combining the component-wise estimates to obtain bounds for $x(t)$ and $u(t)$.

Now for some fixed $i^* \in \mathcal{V}$ we specify an initial condition $x_0 \in \mathbb{R}^n$ such that

$$x_{0,i^*} = \begin{bmatrix} 1 \\ 1 \end{bmatrix} \in \mathbb{R}^2, \quad x_{0,i} = 0 \in \mathbb{R}^2 \quad \text{for all } i \neq i^*.$$

We then employ a model predictive control scheme to numerically approximate the optimal trajectory. To this end, we choose a fixed step size $h > 0$ and perform $N \in \mathbb{N}$ MPC steps until the approximated optimal trajectory satisfies $\|x^*(hN)\| \leq \varepsilon$ for a fixed threshold $\varepsilon > 0$. We then approximate

$$\begin{aligned} \|x^*\|_{L_2}^2 &= \int_0^\infty \|x^*(t)\|^2 dt \approx \int_0^{hN} \|x^*(t)\|^2 dt \\ &\approx h \sum_{k=1}^N \|x^*(hk)\|^2. \end{aligned}$$

The nonlinear MPC controller is implemented using `do-mpc` (see Fiedler et al. (2023)). We consider the case of $s = 25$ vehicles, i.e., $n = 50$, with model parameters $\beta = 5$ and $\kappa = 10$, regularization parameters $\gamma = \delta = 10^{-1}$, and choose $i^* = 12$. Using a step size of $h = 5 \times 10^{-2}$ and a tolerance $\varepsilon = 10^{-4}$, the algorithm terminates after 317 iterations. Figure 2 shows the L_2 -norms of the optimal state trajectories x_i^* for all vehicles $i \in \mathcal{V}$ on a logarithmic scale, for $i^* = 12$ as well as for the cases $i^* \in \{1, 25\}$. The results clearly demonstrate an exponential decay of the trajectory norms with respect to the graph distance, in agreement with Theorem 2.

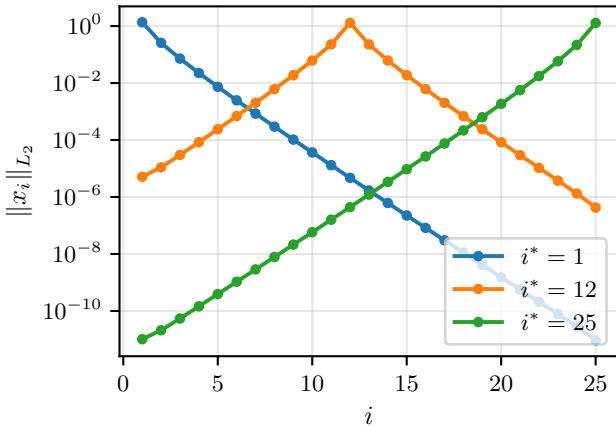


Fig. 2. Decay of the L_2 -norms of the optimal state trajectories x_i for $i^* \in \{1, 12, 25\}$.

6. CONCLUSION

In this paper, we studied spatial decay properties of sensitivities in nonlinear optimal control problems with decoupled dynamics and quadratic cost. Under the assumption of asymptotic controllability to the origin, we established an exponential decay of the sensitivity of the zero solution with respect to the graph distance. For future research, it is of interest to extend the result to nonzero reference trajectories, more general classes of nonlinear dynamics with coupling between subsystems, as well as to broader classes of cost functionals. Further directions include exploring the connection to the decaying sensitivity property of the optimal value function as defined in Sperl et al. (2025).

REFERENCES

Bellman, R. (1957). *Dynamic Programming*. Princeton University Press, Princeton, NJ.

Fiedler, F., Karg, B., Lüken, L., Brandner, D., Heinlein, M., Brabender, F., and Lucia, S. (2023). do-mpc: Towards fair nonlinear and robust model predictive control. *Control Engineering Practice*, 140, 105676.

Grüne, L., Schaller, M., and Schiela, A. (2020). Exponential sensitivity and turnpike analysis for linear quadratic optimal control of general evolution equations. *J. Differential Equations*, 268(12), 7311–7341.

Göttlich, S., Oppeneiger, B., Schaller, M., and Worthmann, K. (2025a). Spatial exponential decay of perturbations in optimal control of general evolution equations. *Preprint arxiv.org/abs/2501.12279*.

Göttlich, S., Schaller, M., and Worthmann, K. (2025b). Perturbations in PDE-constrained optimal control decay exponentially in space. *ESAIM: Control, Optimisation and Calculus of Variations*, 31, 27.

Na, S. and Anitescu, M. (2020). Exponential decay in the sensitivity analysis of nonlinear dynamic programming. *SIAM J. Optim.*, 30(2), 1527–1554.

Oppeneiger, B., Schaller, M., and Worthmann, K. (2025). Spatial decay of perturbations in transport equations with optimal boundary control. *IFAC-PapersOnLine*, 59(8), 66–71.

Qu, G., Wierman, A., and Li, N. (2022). Scalable reinforcement learning for multiagent networked systems. *Oper. Res.*, 70(6), 3601–3628.

Ray, S. and Fröhlich, J. (2015). An analytic solution to the equations of the motion of a point mass with quadratic resistance and generalizations. *Archive of Applied Mechanics*, 85(4), 395–414.

Shin, S., Anitescu, M., and Zavala, V.M. (2022). Exponential decay of sensitivity in graph-structured nonlinear programs. *SIAM J. Optim.*, 32(2), 1156–1183.

Shin, S., Lin, Y., Qu, G., Wierman, A., and Anitescu, M. (2023). Near-optimal distributed linear-quadratic regulator for networked systems. *SIAM J. Control Optim.*, 61(3), 1113–1135.

Shin, S. and Zavala, V.M. (2021). Controllability and observability imply exponential decay of sensitivity in dynamic optimization. *IFAC-PapersOnLine*, 54(6), 179–184.

Slotine, J.J.E. and Li, W. (1991). *Applied nonlinear control*. Prentice-Hall, Englewood Cliffs, NJ.

Sperl, M., Saluzzi, L., Grüne, L., and Kalise, D. (2023). Separable approximations of optimal value functions under a decaying sensitivity assumption. In *2023 62nd IEEE Conference on Decision and Control (CDC)*, 259–264. IEEE.

Sperl, M., Saluzzi, L., Kalise, D., and Grüne, L. (2025). Separable approximations of optimal value functions and their representation by neural networks. *Preprint arxiv.org/abs/2502.08559*. Accepted for publication in *SIAM J. Control Optim.*

Zhang, R.C., Li, W., and Li, N. (2023). On the optimal control of network LQR with spatially-exponential decaying structure. In *2023 American Control Conference (ACC)*, 1775–1780. IEEE.